Regular article

Effect of erbium concentration on optical properties of Er:YLF laser crystals

Jiaqi Hong [a,b,*], Lianhan Zhang [a], Min Xu [a], Yin Hang [a,*]

[a] Key Laboratory of Materials for High Power Laser, Shanghai Institute of Optics and Fine Mechanics, Chinese Academy of Sciences, Shanghai 201800, China
[b] University of Chinese Academy of Sciences, Beijing 100039, China

HIGHLIGHTS

- Four Er-doped LiYF$_4$ crystals with different Er-concentrations were grown.
- Luminescence properties of the four crystals were analyzed in detail.
- Heavily 15 at% Er-doped YLF crystal was found proper in up-conversion or ~3 μm laser applications.

ARTICLE INFO

ABSTRACT

Four Er-doped LiYF$_4$ crystals with different Er-concentrations were grown by Czochralski method. The laser crystals were characterized by measurements of ICP-AES, XRD, absorption spectra, up-conversion fluorescence spectra, near-infrared (NIR) and mid-infrared (Mid-IR) fluorescence spectra, as well as luminescence decays. It was found that the heavily 15 at% Er-doped YLF crystal is more proper in up-conversion or ~3 μm laser applications; while the 5 at% Er-doped YLF is a better candidate for ~1.5 μm lasers within these four crystals.

© 2016 Elsevier B.V. All rights reserved.

1. Introduction

In recent years, laser crystals doped with trivalent erbium ion Er^{3+} have attracted much attentions for their various laser emission wavelengths, including the up-conversions around 550 nm with the transition $^2H_{11/2} + ^4S_{3/2} \rightarrow ^4I_{15/2}$ and around 675 nm with the transition $^4F_{9/2} \rightarrow ^4I_{15/2}$ as well as the near-IR lasers around 1.5 μm with the transition $^4I_{13/2} \rightarrow ^4I_{15/2}$ and the mid-IR (MIR) lasers around 2.7 μm with the transition $^4I_{11/2} \rightarrow ^4I_{13/2}$ [1–7]. Moreover, the Lasers around 1.5 and 2.7 μm are useful for telecommunication, long-distance telemetry and ranging, medicine, coherent LIDAR and the generation of longer wavelengths via optical parametric oscillators (OPOs) [8–11].

Several oxide and fluoride crystals, such as YAG, YAP, LiYF$_4$, LiLuF$_4$ and CaF$_2$, have been proposed for Er doping, and some related studies have been carried out to investigate the properties of these Er-doped crystals [5–9,12–14]. Compared with oxides, fluoride crystals are more attractive due to their high transparency in a wide wavelength range from the vacuum ultraviolet (VUV) to the infrared (IR) as well as their low phonon-energy that reduces non-radiative relaxation between adjacent energy levels and increases upper laser level lifetime. In addition, fluoride crystals benefit from lower refractive index, which together with other thermo-optical properties limits non-linear effects under intense laser pumping. One of the most widely used fluoride crystals is LiYF$_4$, which besides the favorable properties above is also characterized by a negative thermal dependence of refractive index that compensates the positive thermal expansion coefficients to significantly weaken thermal lensing.

Up to now, sufficient works have been done on the spectroscopy and laser operations of Er doped LiYF$_4$ [14–19], but with no research concerning the influence of different Er doping concentrations to the crystal optical properties. Therefore, a systematically complete study of the optical characterization of Er:YLF with different doping levels is necessary to fully understand the performance of Er^{3+} in YLF crystals and contribute to optimizing its laser output.

In this work, we have performed spectral analyses on four differently Er-doped YLF crystals, based on measurements of the

---

* Corresponding authors at: Key Laboratory of Materials for High Power Laser, Shanghai Institute of Optics and Fine Mechanics, Chinese Academy of Sciences, Shanghai 201800, China (J. Hong).

E-mail addresses: hongjiaqi@siom.ac.cn (J. Hong), yhang@siom.ac.cn (Y. Hang).

Table 1
Concentrations of the dopant ions at the growth starting position in the as-grown crystals and in the melt.

| Samples	1.5 at% Er:YLF	3 at% Er:YLF	5 at% Er:YLF	15 at% Er:YLF
C_0 of Er (wt%)	1.45	2.88	4.76	13.67
C_s of Er (wt%)	1.34	2.72	4.60	13.49
C_s of Er (10^{20} cm^{-3})	1.19	3.77	6.37	18.67
K_0 of Er	0.92	0.94	0.97	0.99
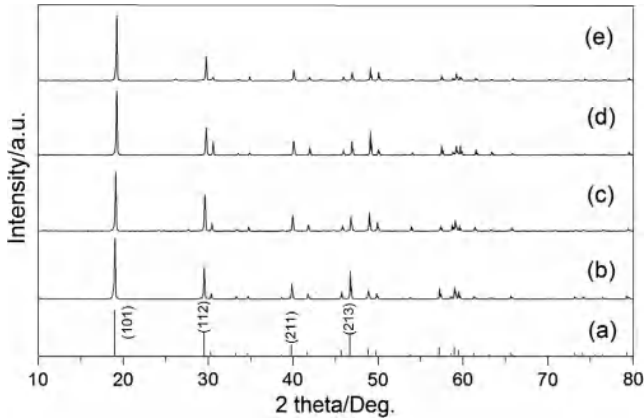
Fig. 1. (a) XRD pattern of pure LiYF$_4$ crystal from the PDF database, no. 17-0874 and XRD patterns of (b) 1.5 at%, (c) 3 at%, (d) 5 at%, (e) 15 at% Er:YLF.

ICP-AES, XRD, absorption spectra, up-conversion fluorescence spectra, near-infrared and mid-infrared fluorescence spectra, as well as luminescence decay curves.

2. Experiments

The four Er:YLF single crystals were grown in a Czochralski system with intermediate frequency induction heating and an automated diameter-control equipment by monitoring the weight of the crystals. The starting materials were commercially available fluoride powders of LiF, YF$_3$ and ErF$_3$, each with high purity of 99.99%. The concentrations of Er in the raw materials were 1.5 at %, 3 at%, 5 at% and 15 at%. Before crystal growth, the chamber was firstly evacuated to 10^{-3} Pa, and then slowly injected with high-purity CF$_4$ gas (99.9999%) as protective atmosphere during the whole growth procedure. Each crystal was grown by using an α-axis oriented un-doped YLF seed crystal with the pulling rate of 1 mm/h and the rotation rate of 15 r/min. After growth, each
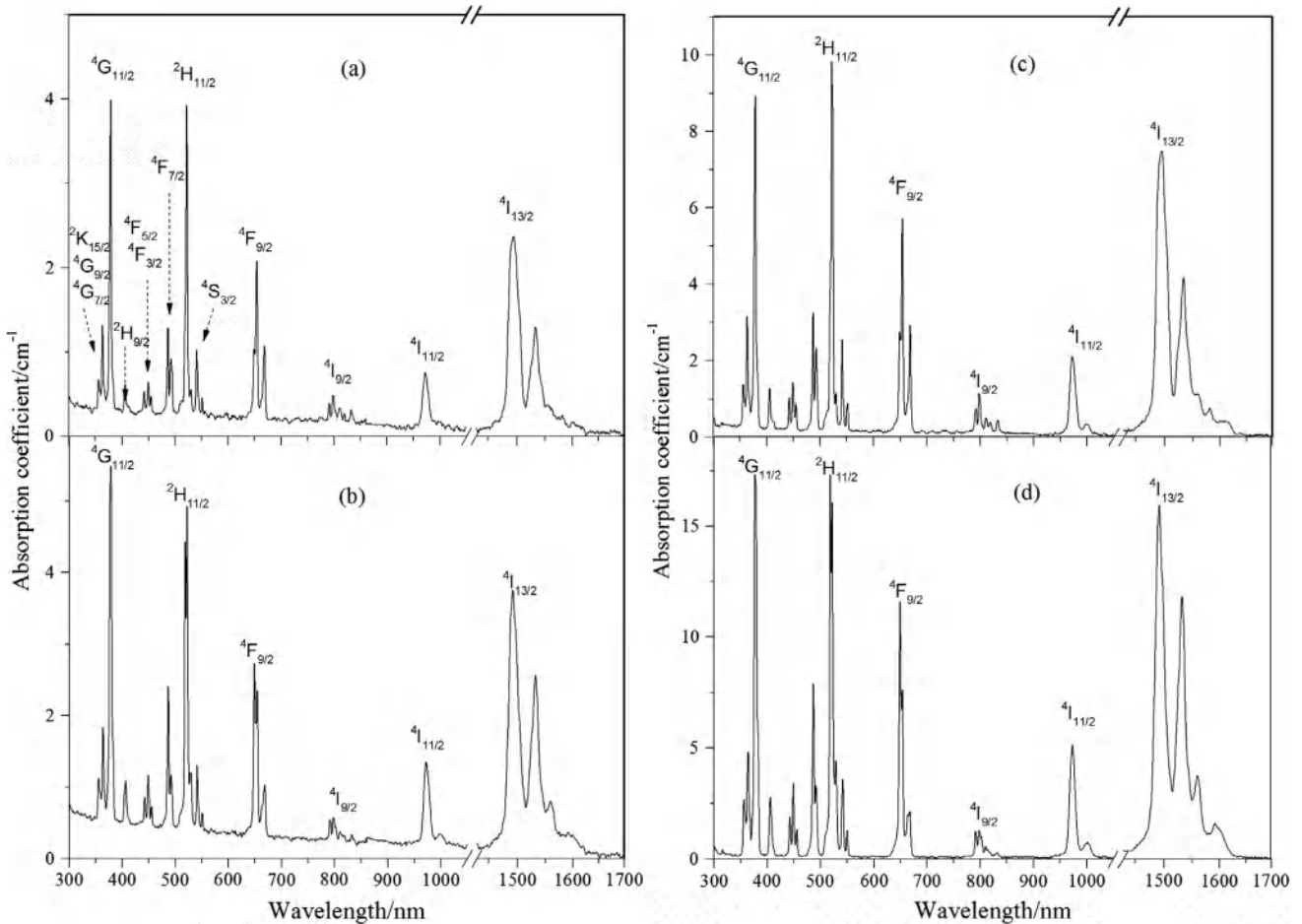
Fig. 2. Absorption spectra of (a) 1.5 at%, (b) 3 at%, (c) 5 at%, (d) 15 at% Er:YLF.
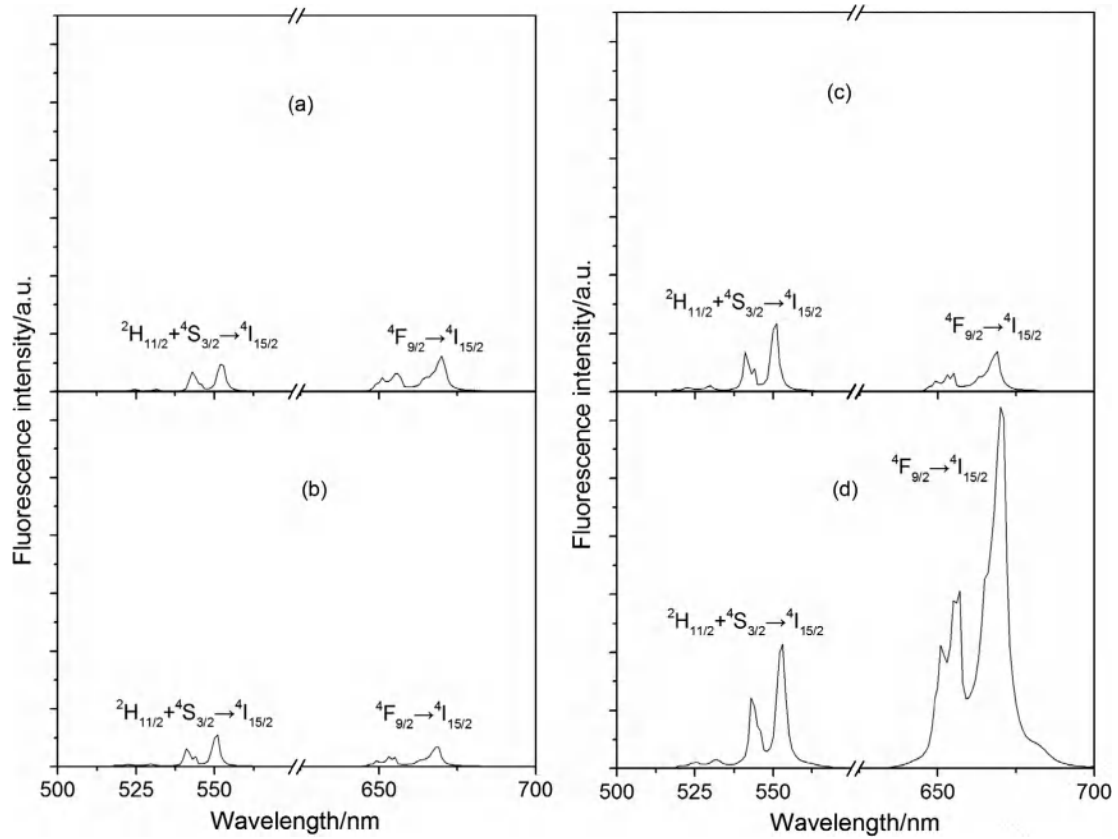
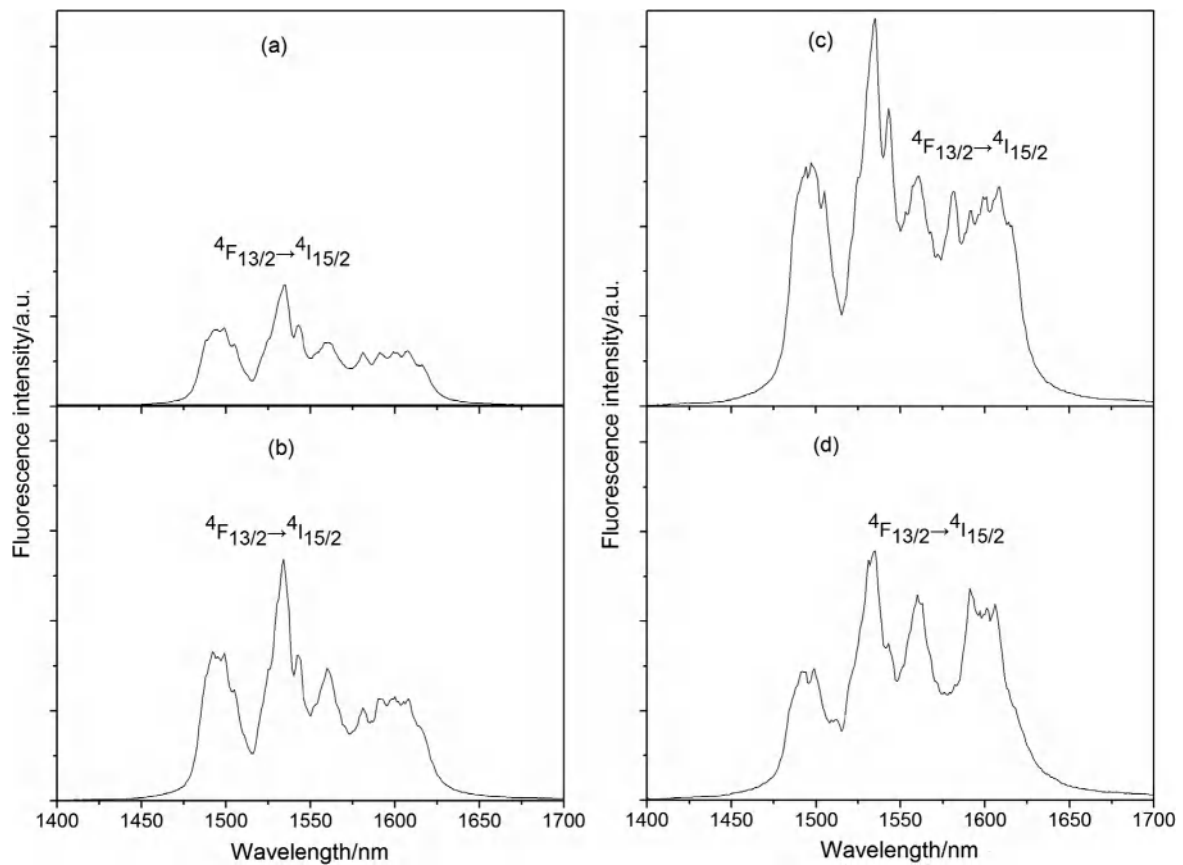**Fig. 3.** Up-conversion fluorescence spectra of (a) 1.5 at%, (b) 3 at%, (c) 5 at%, (d) 15 at% Er:YLF.

Fig. 4. NIR fluorescence spectra of (a) 1.5 at%, (b) 3 at%, (c) 5 at%, (d) 15 at% Er:YLF.
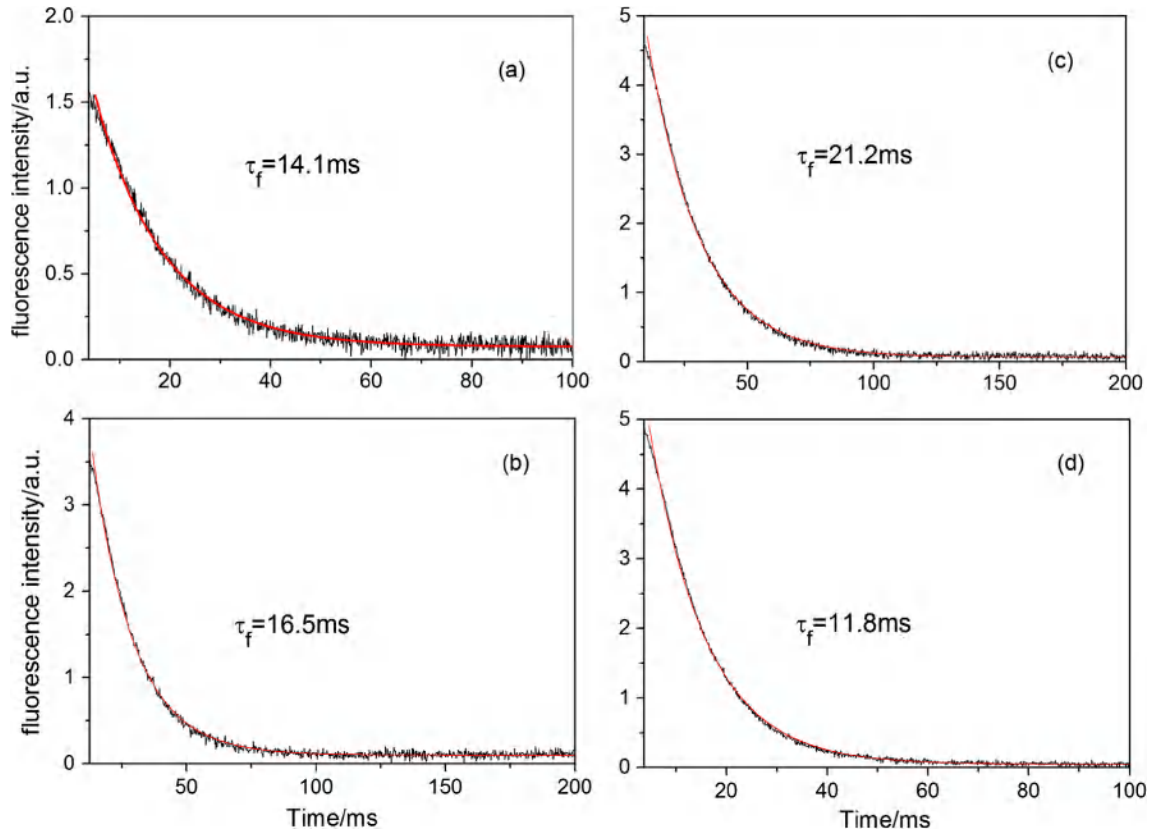
Fig. 5. Fluorescence decay curves of Er^{3+}:$^4I_{13/2}$ manifold in the (a) 1.5 at%, (b) 3 at%, (c) 5 at%, (d) 15 at% Er:YLF.

crystal was cooled down to room temperature at a rate of 30–50 °C/h.

In the following experiments, the segregation coefficients of the Er^{3+} in the Er:YLF crystals were detected by inductively coupled plasma-atomic emission spectrometry (ICP-AES). The crystal structure identifications were undertaken on a D/max2550 X-ray diffraction (XRD) using Cu Kα radiation. Samples of Φ 30 mm for spectroscopic measurements were cut from the as-grown bulk crystals with faces perpendicular to the [1 0 0] crystallographic direction and mechanically polished to spectral quality with thickness of 1 mm for absorption measurements and 0.5 mm for fluorescence measurements. The absorption spectra were recorded by a UV–vis-NIR spectrophotometer (Lambda-900) in the range of 300–1700 nm with non-polarized incident light. The up-conversion fluorescence spectra within 500–700 nm, the fluorescence spectra in the ranges of 1400–1700 nm and 2550–2850 nm as well as the relevant decay curves were all recorded under excitation of 976 nm by Edinburg Instruments FLSP920 spectrophotometer. All of the crystal growth, the spectroscopic measurements were made with the same experimental set-ups to reduce the influences of the conditions and apparatus differences.

3. Results and discussions

The 1.5 at%, 3 at%, 5 at% and 15 at% Er^{3+}:YLF crystals of about $\Phi 30 \times 40$ mm^3 are all successfully grown without cracks, bubbles, and inclusions. The segregation coefficients K_0 of Er^{3+} can be calculated from the following formula: $K_0 = C_s/C_0$, where C_s is the dopant ion concentration at the growth starting position in the as-grown

crystals and C_0 is the dopant ion concentration in the melt. The C_s of the doped Er^{3+} ion in the crystals are measured by ICP-AES, as listed in Table 1. Each K_0 approximately equals to 1, indicating that Er^{3+} ions can be uniformly distributed in the YLF crystal lattice, which is because that the ionic radius of Er^{3+} (0.0881 nm) is so close to that of Y^{3+} (0.088 nm).

The XRD patterns of the as-grown four Er:YLF crystals and the un-doped LiYF$_4$ crystal from the PDF database, no. 17-0874, are shown in Fig. 1. The diffraction peaks of each crystal are strong and no second phase diffraction peak is found, indicating that the as-grown crystals are well-crystallized and the impurities do not change the essential structure of LYF. The lattice parameters of the 1.5, 3, 5 and 15 at% Er^{3+}:YLF crystals are respectively determined to be (a = 0.5173 nm, c = 1.0747 nm), (a = 0.5169 nm, c = 1.0732 nm), (a = 0.5158 nm, c = 1.0708 nm) and (a = 0.5156 nm, c = 1.0714 nm), all of which are slightly changed with those of the pure LYF crystal (a = 0.5168 nm, c = 1.0709 nm), and the phenomenon can be explained by the ionic radius difference of Er^{3+} (0.089 nm) and Y^{3+} (0.09 nm).

The room temperature absorption spectra are shown in Fig. 2, and the absorption coefficient is calculated by $\alpha = A/(L \times \log e)$, where A is the absorbance and L is the thickness of the polished crystal samples [20]. The absorption peaks corresponding to the transitions from the ground state $^4I_{15/2}$ to the excited states of Er^{3+} ions are marked in the figure. The center wavelengths of absorption peaks scarcely change for different Er^{3+} doping levels, while intensity of absorption peaks significantly increase with increasing Er^{3+} concentrations. There is one relatively strong absorption band located around 980 nm, which well matches the emitting wavelength of high-power InGaAs laser diodes.
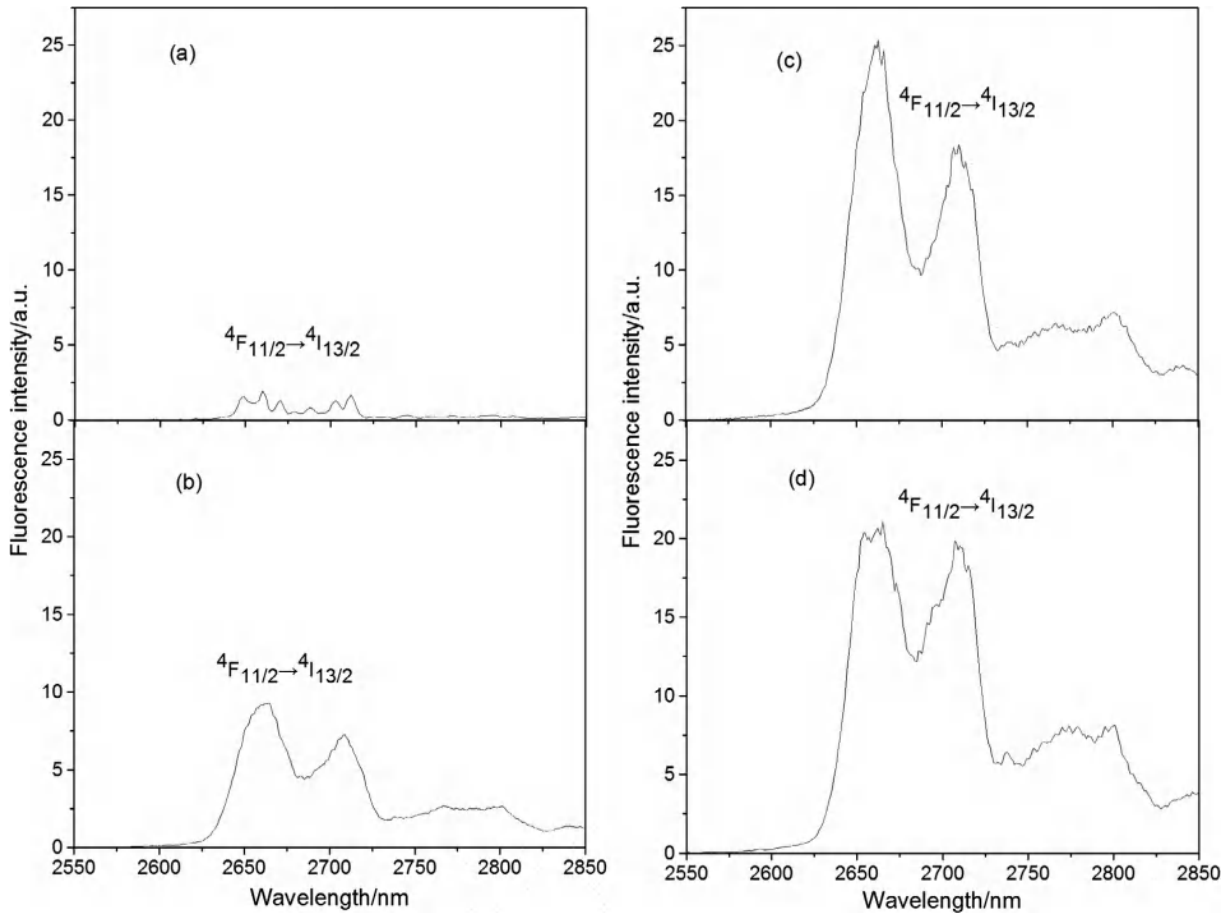
Fig. 6. Mid-IR fluorescence spectra of (a) 1.5 at%, (b) 3 at%, (c) 5 at%, (d) 15 at% Er:YLF.

The up-conversion fluorescence spectra of the four crystals in the 500–700 nm wavelength range are presented in Fig. 3. Green and red emission bands are observed with peaks at around 543, 552 nm and 650, 657, 670 nm, corresponding to $^2H_{11/2}$ + $^4S_{3/2} \rightarrow {}^4I_{15/2}$ and $^4F_{9/2} \rightarrow {}^4I_{15/2}$ transitions, respectively. The green emissions strengthen gradually as the Er^{3+} concentration increases from 1.5 to 15 at%. The red emission intensities scarcely change with the doping concentrations of 1.5, 3 and 5 at%, but increases dramatically with 15 at% Er-doping. Furthermore, the green luminescence is comparable to or slightly weaker than the red luminescence with the doping concentrations of 1.5, 3 and 5 at%. However, for 15 at% doping, the intensity of the red luminescence is obviously stronger than that of the green luminescence. It seems the heavily 15 at% Er-doped YLF crystal is better when applied in up-conversion lasers.

The NIR fluorescence spectra in the wavelength range of 1400–1700 nm are shown in Fig. 4. The fluorescence band ranges wide from 1475 to 1625 nm and centers at around 1534 nm, corresponding to the $^4I_{13/2} \rightarrow {}^4I_{15/2}$ transition. It can be seen that the fluorescence intensity increases considerably with increase of Er-concentrations from 1.5 to 5 at%. However, the 15 at% Er:YLF shows an opposite trend, which can be explained by concentration quenching and self-reabsorption because of high Er-concentration. Moreover, with heavily Er-doping, reabsorption effect can also distort the emission spectrum as Fig. 4(d) shows.

The fluorescence decay curves of Er^{3+}:$^4I_{13/2}$ manifold in four Er:YLF crystals are shown in Fig. 5. The relationships in the figure all present single exponential decay behaviors, and the fluorescence

lifetimes τ_f are measured to be 14.1, 16.5, 21.2 and 11.8 ms for the 1.5, 3, 5 and 15 at% Er:YLF, respectively, which just show a similar trend as the NIR fluorescence spectra above. Therefore, with the strongest fluorescence intensity and the longest fluorescence lifetime, the 5 at% Er-doped YLF seems a best candidate for ~1.5 μm lasers within these four crystals.

The Mid-IR fluorescence spectra in the wavelength range of 2550–2850 nm are shown in Fig. 6. Emission peaks at around 2663, 2709, 2766, 2800 and 2843 nm are observed, which assign to the $^4I_{11/2} \rightarrow {}^4I_{13/2}$ transition. It can be seen that the emission intensity increases with the increase of Er-concentrations from 1.5 to 5 at%, while the fluorescence intensities of the 5 and 15 at% Er:YLF are rather comparable.

The fluorescence decay curves of the Er^{3+}:$^4I_{11/2}$ manifold in four Er:YLF crystals are shown in Fig. 7. The relationships in the figure all present single exponential decay behaviors, and the fluorescence lifetimes τ_f are measured to be 3.58, 4.13, 4.27 and 2.61 ms for the 1.5, 3, 5 and 15 at% Er:YLF, respectively. Although the fluorescence lifetime of $^4I_{13/2}$ manifold decreases with 15 at% Er-doping, it can be seen that self-termination problem for $^4I_{11/2} \rightarrow {}^4I_{13/2}$ transition still exist because the lifetime of $^4I_{11/2}$ manifold decreases as well and τ_f ($^4I_{11/2}$) is still shorter than τ_f ($^4I_{13/2}$). However, it is found that lifetime of $^4I_{11/2}$ manifold decreases a little faster than that of the $^4I_{13/2}$ manifold for 15 at% Er-doping, which is favorable for overcoming the population "bottleneck" effect [13] and benefit for the ~3 μm laser operations. Thus, it seems that the heavily 15 at% Er-doped YLF crystal is more proper for ~3 μm laser applications.
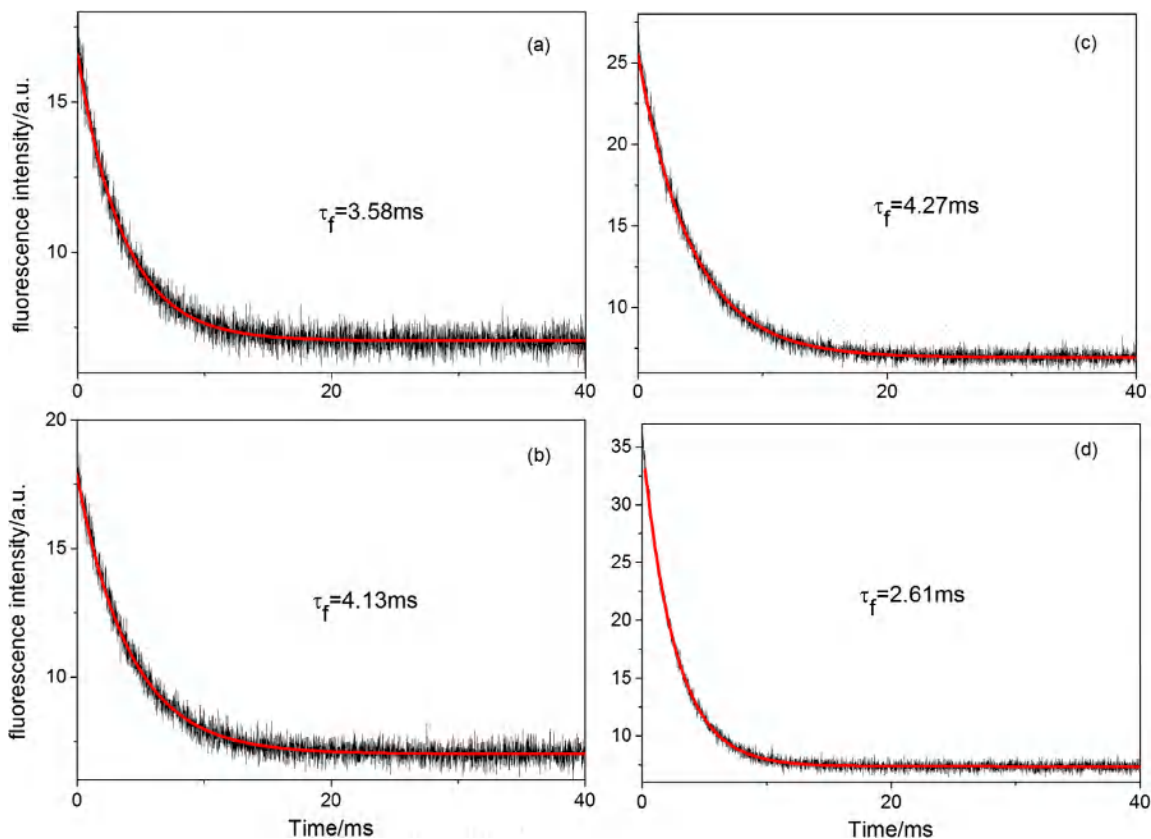
Fig. 7. Fluorescence decay curves of Er^{3+}:$^4I_{11/2}$ manifold in the (a) 1.5 at%, (b) 3 at%, (c) 5 at%, (d) 15 at% Er:YLF.

4. Conclusion

Four 1.5 at%, 3 at%, 5 at%, and 15 at% Er^{3+}-doped $LiYF_4$ crystals were grown by Czochralski method. ICP-AES and XRD studies show that segregation coefficient of Er^{3+} of each crystal approximately equals to 1, and the Er-doping do not change the essential structure of LYF. Spectroscopic properties of four crystals were detailed investigated by measurements of absorption spectra, up-conversion fluorescence spectra, near-infrared (NIR) and mid-infrared (Mid-IR) fluorescence spectra, as well as luminescence decays of the $^4I_{11/2}$ and $^4I_{13/2}$ manifolds. It was found that the heavily 15 at% Er-doped YLF crystal is more suitable for up-conversion or ~3 μm laser applications; while the 5 at% Er-doped YLF is a better candidate for ~1.5 μm lasers within these four crystals.

Acknowledgements

References

[1] Hai Guo, Green and red upconversion luminescence in CeO_2:Er^{3+} powders produced by 785 nm laser, J. Solid State Chem. 180 (2007) 127–131.

[2] Tirtha Som, Basudeb Karmakar, Efficient green and red fluorescence upconversion in erbium doped new low phonon antimony glasses, Opt. Mater. 31 (2009) 609–618.

[3] X.F. Yang, Y. Wang, H.T. Huang, D.Y. Shen, D.Y. Tang, H.Y. Zhu, X.D. Xu, D.H. Zhou, J. Xu, A passively Q-switched Er:LuYAG laser with a graphene saturable absorber, Laser Phys. Lett. 10 (2013) 105810.

[4] K.N. Gorbachenya, V.E. Kisel, A.S. Yasukevich, V.V. Maltsev, N.I. Leonyuk, N.V. Kuleshov, Eye-safe 1.55 μm passively Q-switched Er, Yb:GdAl₃(BO₃)₄ diode-pumped laser, Opt. Lett. 41 (2016) 918–921.

[5] B.Q. Yao, T.Y. Dai, Deng, X.M. Duan, Y.L. Ju, Y.Z. Wang, Tunable single-longitudinal-mode Er:YAG laser using a twisted-mode technique at 1.6 μm, Laser Phys. Lett. 12 (2015) 025004.

[6] Manuel Messner, Arne Heinrich, Clemens Hagen, Karl Unterrainer, High brightness diode pumped Er:YAG laser system at 2.94 μm with nearly 1 kW peak power, Proc. SPIE 9726 (2016) 972602.

[7] K.N. Gorbachenya, S.V. Kurilchik, V.E. Kisel, A.S. Yasukevich, N.V. Kuleshov, A.S. Nizamutdinov, S.L. Korableva, V.V. Semashko, Laser performance of in-band pumped Er:LiYF₄ and Er:LiLuF₄ crystals, Quantum Elect. 46 (2016) 95–99.

[8] M. Skorczakowski, J. Swiderski, W. Pichola, P. Nyga, A. Zajac, M. Maciejewska, L. Galecki, J. Kasprzak, S. Gross, A. Heinrich, T. Bragagna, Mid-infrared Q-switched Er:YAG laser for medical applications, Laser Phys. Lett. 7 (2010) 498–504.

[9] X. Wang, H. Fritsche, O. Lux, H.J. Eichler, Z.G. Zhao, Casey Schuett, Bastian Kruschke, Dual-wavelength Q-switched Er:YAG laser around 1.6 μm for methane differential absorption lidar, Laser Phys. Lett. 10 (2013) 115804.

[10] P.E. Britton, H.L. Offerhaus, D.J. Richardson, P.G.R. Smith, G.W. Ross, D.C. Hanna, Parametric oscillator directly pumped by a 1.55-μm erbium-fiber laser, Opt. Lett. 24 (1999) 975–977.

[11] Marco Vitiello, Andrea Pizzarulli, Andrea Ruffini, A compact high power Er: Yb:glass eye safe laser for infrared remote sensing applications, Proc. SPIE 7836 (2010) 78360C.

[12] Ningning Zu, Haigui Yang, Zhenwen Dai, Different processes responsible for blue pumped, ultraviolet and violet luminescence in high-concentrated Er^{3+}: YAG and low-concentrated Er^{3+}:YAP crystals, Phys. B 403 (2008) 174–177.

[13] Weiwei Ma, Liangbi Su, Xiaodong Xu, Jingya Wang, Dapeng Jiang, Lihe Zheng, Xiuwei Fan, Chun Li, Jie Liu, Jun Xu, Effect of erbium concentration on spectroscopic properties and 2.79 μm laser performance of Er:CaF_2 crystals, Opt. Mater. Express 6 (2016) 409–415.

[14] F. Moglia, Upconversion lasers and other applications of Er^{3+}-doped fluoride crystals, 2014.

[15] Marly B. Camargo, Laercio Gomes, Izilda M. Ranieri, Concentration effects on the IR-luminescent channels for Er- and Ho-doped $LiYF_4$ crystals, Opt. Mater. 6 (1996) 331–338.

[16] Octavian Toma, Serban Georgescu, Competition between green and infrared emission in Er:YLiF₄ upconversion lasers, Opt. Commun. 284 (2011) 388–397.

[17] T. Jensen, A. Diening, G. Huber, Investigation of diode-pumped 2.8-μm Er:LiYF₄ lasers with various doping levels, Opt. Lett. 21 (1996) 585–587.

[18] Alex Dergachev, Peter F. Moulton, Tunable CW Er:YLF Diode-Pumped Laser, OSA/ASSP, 2003.

[19] F. Heine, E. Heumann, T. Danger, T. Schweizer, G. Huber, B. Chai, Green upconversion continuous wave Er^{3+}:LiYF₄ laser at room temperature, Appl. Phys. Lett. 65 (1994) 383–384.

[20] Yan Wang, Zhenyu You, Jianfu Li, Zhaojie Zhu, En Ma, Chaoyang Tu, Spectroscopic investigations of highly doped Er^{3+}:GGG and Er^{3+}/Pr^{3+}:GGG crystals, J. Phys. D: Appl. Phys. 42 (2009) 215406.